

Scientific paper

# Ionic conductance of Lithium Exchanged Phases in Amorphous and Crystalline Zirconium Titanium Phosphate

Rakesh Thakkar and Uma Chudasama\*

Applied Chemistry Department, Faculty of Technology and Engineering, The M. S. University of Baroda, Vadodara – 390 001, Gujarat, India

\* Corresponding author: E-mail: uvces@gmail.com

Received: 29-09-2008

## Abstract

Lithium exchanged phases of amorphous and crystalline zirconium titanium phosphate have been synthesized by an ion exchange technique. These materials have been characterized by elemental analysis (ICP-AES and AAS), spectral analysis (FTIR), thermal analysis (TGA) and X-ray diffraction studies. The conductance properties of these materials have been explored by measuring specific conductance at different temperatures in the range of 30–250 °C at 10 °C intervals, using impedance analyzer over a frequency range 1 Hz – 32 MHz at a signal level below 1 V. Lithium exchanged phases of amorphous and crystalline zirconium phosphate and titanium phosphate have also been synthesized under identical conditions, characterized and their conductance properties investigated for comparative studies. It is observed that, in all cases, conductivity decreases with increasing temperature. Conductance performance is discussed based on conductivity data and activation energy.

**Keywords:** Solid electrolyte, ionic conductor, lithium ion conductor, tetravalent metal acid salts, zirconium titanium phosphate, lithium exchanged phases of zirconium titanium phosphate.

## 1. Introduction

Tetravalent metal acid (TMA) salts possess the general formula  $M(IV)(HXO_4)_2 \cdot nH_2O$  where  $M(IV) = Zr, Ti, Sn, Ce, Th$  etc and  $X = P, Mo, W, As, Sb$  etc. The protons present in the structural hydroxyl groups of these materials can be exchanged for several cations with retention of basic structure and properties. TMA salts have been widely investigated for proton transport behaviour.<sup>1,2</sup> Proton conductors find applications in fuel cells, sensors, water electrolysis units and other electrochemical devices.

Metal exchanged phases ( $Li^+, Na^+, K^+, Ag^+, Ni^{2+}, Cu^{2+}$ ) of TMA salts have been investigated for ion conduction behaviour.<sup>3,4,5</sup> Lithium ion conductors are especially attractive. Small ionic radius and lower weight of lithium ion, being essential criteria for good conduction, besides an extremely high reduction potential of lithium ion supports its potential use in high energy density batteries. Further, lithium ion transport is promoted in cation exchange materials.<sup>6</sup>

Conductivity of lithium exchanged tin phosphate<sup>7,8</sup> and zirconium phosphate<sup>9</sup> have been reported. Lithium exchanged iron (III) phosphate has been investigated for rechargeable lithium-ion battery application.<sup>10</sup>  $Li_9M_3(P_2O_7)_3(PO_4)_2$  with  $M = Al, Ga, Cr, Fe$  was synthesized and their transport properties investigated.<sup>11</sup> Transport properties of  $Li^+$  and  $Cu^{2+}$  exchanged phases of zirconium phosphate have been reported by us.<sup>12</sup> It has also been observed that amorphous phases of TMA salts exhibit higher conductance compared to corresponding crystalline phases,<sup>13</sup> and mixed materials exhibit higher conductance compared to their single salt counter parts.<sup>14</sup>

In the light of above studies, in the present endeavor, lithium exchanged phases of amorphous and crystalline zirconium titanium phosphate (LiZTPA, LiZTPC) have been synthesized. These materials have been characterized by elemental analysis (ICP-AES and AAS), spectral analysis (FTIR), thermal analysis (TGA) and X-ray diffraction studies. The conductance properties of these ma-

materials have been explored by measuring specific conductance at different temperatures in the range of 30–250 °C at 10 °C intervals, using Solartron Impedance Analyzer (SI 1260) over a frequency range 1 Hz – 32 MHz at a signal level below 1 V. Lithium exchanged phases of single salt counter parts, both amorphous and crystalline, zirconium phosphate (LiZPA, LiZPC) and titanium phosphate (LiTPA, LiTPC) have also been synthesized under identical conditions, characterized, their conductance properties investigated for comparative studies and conductance performance discussed based on conductivity data and activation energy.

## 2. Experimental

### 2.1 Synthesis of Zirconium Titanium Phosphate – Amorphous (ZTPA)

A solution containing 0.1 M  $\text{ZrOCl}_2 \cdot 8\text{H}_2\text{O}$  and 0.1 M  $\text{TiCl}_4$  in 10 % w/v  $\text{H}_2\text{SO}_4$  (100 mL) was prepared. To this solution 200 mL, 0.2 M  $\text{NaH}_2\text{PO}_4 \cdot 2\text{H}_2\text{O}$  was added dropwise (flow-rate, 1 mL  $\text{min}^{-1}$ ) with continuous stirring at room temperature. After complete precipitation, the obtained gel was stirred for another 5 h. The precipitate was kept in contact with mother liquor overnight, filtered, washed with double distilled water to remove adhering ions (chloride and sulfate) {stage 1} and dried at room temperature. The material was then broken down to the desired particle size [30–60 mesh (ASTM)] by grinding and sieving. 5 g of this material was treated with 50 mL of 1M  $\text{HNO}_3$  for 30 min with occasional shaking. The sample was then separated from acid by decantation and treated with double distilled water to remove adhering acid. This process (acid treatment) was repeated at least five times. After final washing, the material was dried at room temperature.

### 2.2 Synthesis of Zirconium Phosphate – Amorphous (ZPA) and Titanium Phosphate – Amorphous (TPA)

A solution of  $\text{ZrOCl}_2 \cdot 8\text{H}_2\text{O}$  (0.1 M, 100 mL) or  $\text{TiCl}_4$  (0.1 M, 100 mL) in 10 % w/v  $\text{H}_2\text{SO}_4$  was prepared as the case may be. To this solution  $\text{NaH}_2\text{PO}_4 \cdot 2\text{H}_2\text{O}$  (0.2 M, 200 mL) was added dropwise (flow-rate, 1 mL  $\text{min}^{-1}$ ) with continuous stirring at room temperature. After complete precipitation, the obtained gel was stirred for another 5 h. The precipitates was kept in contact with mother liquor overnight, filtered, washed with double distilled water to remove adhering ions (chloride and sulfate) {stage 1} and dried at room temperature. The materials were then broken down to the desired particle size [30–60 mesh (ASTM)] by grinding and sieving. The material was acid treated as in 2.1.

### 2.3. Synthesis of Zirconium Titanium Phosphate – Crystalline (ZTPC), Zirconium Phosphate – Crystalline (ZPC) and Titanium Phosphate – Crystalline (TPC)

The gel obtained in stage 1, (as in 2.1, 2.2) above was refluxed with phosphoric acid for ~ 100 h, filtered, washed and dried at room temperature to obtain the crystalline material.

### 2.4. Lithium Exchanged Phases

2 g of each material (ZTPA, ZPA, TPA, ZTPC, ZPC, TPC) was equilibrated with 200 mL, 0.2 M lithium acetate solution, with continuous stirring at 50 °C for 100 h. The solid was separated by filtration and washed with conductivity water for removal of adhering ions and dried at room temperature. Lithium exchanged phases of amorphous and crystalline phases are abbreviated as Li-ZTPA, LiZPA, LiTPA and LiZTPC, LiZPC, LiTPC and respectively.

### 2.5. Instrumentation

The samples were analyzed for zirconium, titanium and phosphorus content using ICP-AES (Labtam, 8440 Plasmalab) and lithium content by AAS (Chemito, AA203). X-ray diffractogram ( $2\theta = 5\text{--}80^\circ$ ) was obtained on X-ray diffractometer (Bruker AXS D8) with  $\text{Cu-K}\alpha$  X-ray source of wavelength 1.5418 Å and nickel filter. FTIR spectra were recorded using KBr wafer on a Perkin Elmer Paragon 1000 spectrophotometer. Thermal analysis (TGA) was carried out on a Shimadzu DT 30 thermal analyzer at a heating rate of 10 °C  $\text{min}^{-1}$ . Solartron Impedance Analyzer (SI 1260) was used for specific conductance measurement.

### 2.6. Conductivity Measurements

The proton conductivity of the materials was measured using pellets of 10 mm diameter and 1.5–2.0 mm thickness. Pellets were prepared by pressing ~ 300 mg of material at 40 KN/cm<sup>2</sup>. The two opposite flat surfaces of the pellets were coated with conducting silver paste to ensure good electrical contacts. Complex impedance was measured in the temperature range 30–250 °C, at 10 °C intervals, using Solartron Impedance Analyzer (SI 1260) over a frequency range 1 Hz – 32 MHz at a signal level below 1 V, interfaced to a computer for data collection. In all cases, since the impedance plots of the materials consist of single depressed semicircle, the pellet conductivity was calculated by arc extrapolation to the real axis, taking into account the geometrical sizes of the pellets.

### 3. Results and Discussion

#### 3. 1. Characterization

LiZPA, LiTPA, LiZTPA are obtained as white hard granules while LiZPC, LiTPC and LiZTPC are obtained as white powder. Elemental analysis performed by ICP-AES shows M : P ratio as 1 : 1 in LiZPA, LiTPA, LiZPC and LiTPC. Zr : Ti : P ratio is found to be 1 : 1 : 2 in LiZTPA and LiZTPC. For all characterizations (X-ray, FTIR, thermal), as a representative, figures of LiZTPA and LiZTPC are presented.

The absence of any sharp peaks in the X-ray diffractograms of LiZTPA (Fig. 1a) indicates amorphous nature of the material. Sharp peaks obtained in case of LiZTPC (Fig. 1b) indicate crystalline nature of the materials. The X-ray diffractogram of LiZPA and LiTPA also does not exhibit any peak indicating amorphous nature of the material. The crystalline phases of LiZPC and LiTPC were confirmed from the JCPDS card no. 33-1482 and 44-0382 respectively.

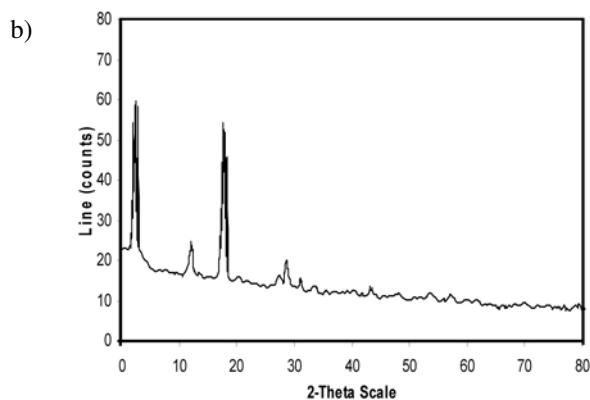
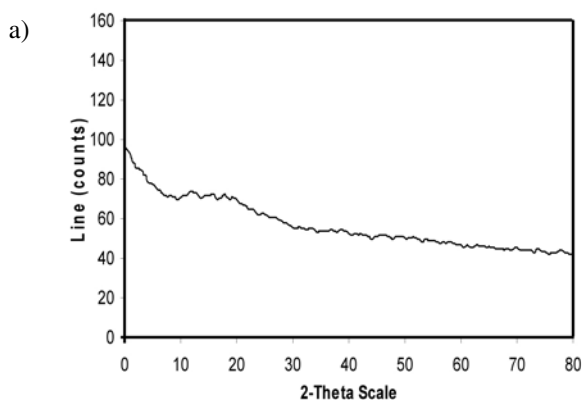


Fig. 1. X ray diffractograms of (a) LiZTPA and (b) LiZTPC.

The FTIR spectra (Fig. 2a,b) exhibit a broad band in the region  $\sim 3400\text{ cm}^{-1}$  which is attributed to asymmetric and symmetric  $-\text{OH}$  stretches. A sharp medium band at

$1620\text{ cm}^{-1}$  is attributed to aquo (H–O–H) bending. A band in the region  $\sim 1035\text{ cm}^{-1}$  is attributed to the presence of P=O stretching. A medium intensity band at  $1400\text{ cm}^{-1}$  is attributed to the presence of  $\delta(\text{POH})$ .<sup>15</sup> These bands indicate the presence of structural hydroxyl groups/protonic sites in the material. No characteristic changes are observed in the FTIR spectrum of the lithium exchanged phases. However, additional metal-oxygen stretches, Li–O have been observed<sup>16</sup>  $\sim 526\text{ cm}^{-1}$ , confirming the formation of lithium exchanged phases.

TGA of all the materials (Fig. 3a,b) indicates two weight loss regions. The first weight loss region (up to  $\sim 180\text{ }^\circ\text{C}$ ) is attributed to loss of moisture/hydrated water. The second weight loss in the range  $250\text{--}500\text{ }^\circ\text{C}$  is attributed to condensation of structural hydroxyl groups.

Based on the elemental analysis (ICP-AES and AAS) and thermal analysis (TGA) data, LiZPA, LiTPA, LiZTPA, LiZPC, LiTPC, LiZTPC, are formulated as

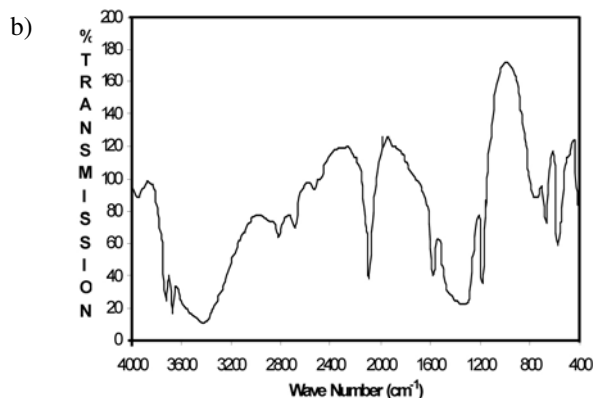
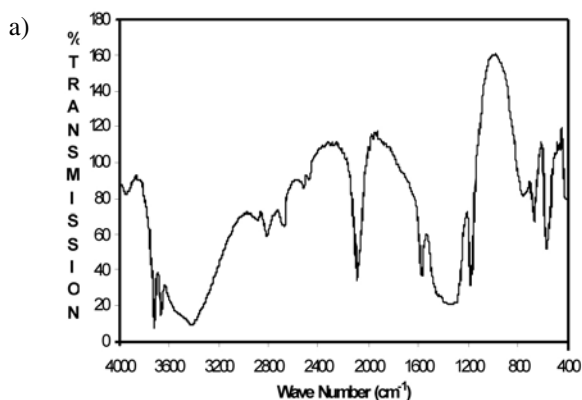


Fig. 2. FTIR spectra of (a) LiZTPA and (b) LiZTPC.

$\text{ZrLi}_{0.51}\text{H}_{1.49}(\text{PO}_4)_2 \cdot 2\text{H}_2\text{O}$ ,  $\text{TiLi}_{0.57}\text{H}_{1.43}(\text{PO}_4)_2 \cdot 2.5\text{H}_2\text{O}$  and  $\text{Zr}_{0.55}\text{Ti}_{0.45}\text{Li}_{0.62}\text{H}_{1.38}(\text{PO}_4)_2 \cdot \text{H}_2\text{O}$ ,  $\text{ZrLi}_{0.49}\text{H}_{1.51}(\text{PO}_4)_2 \cdot \text{H}_2\text{O}$ ,  $\text{TiLi}_{0.52}\text{H}_{1.48}(\text{PO}_4)_2 \cdot \text{H}_2\text{O}$  and  $\text{Zr}_{0.51}\text{Ti}_{0.49}\text{Li}_{0.58}\text{H}_{1.42}(\text{PO}_4)_2$

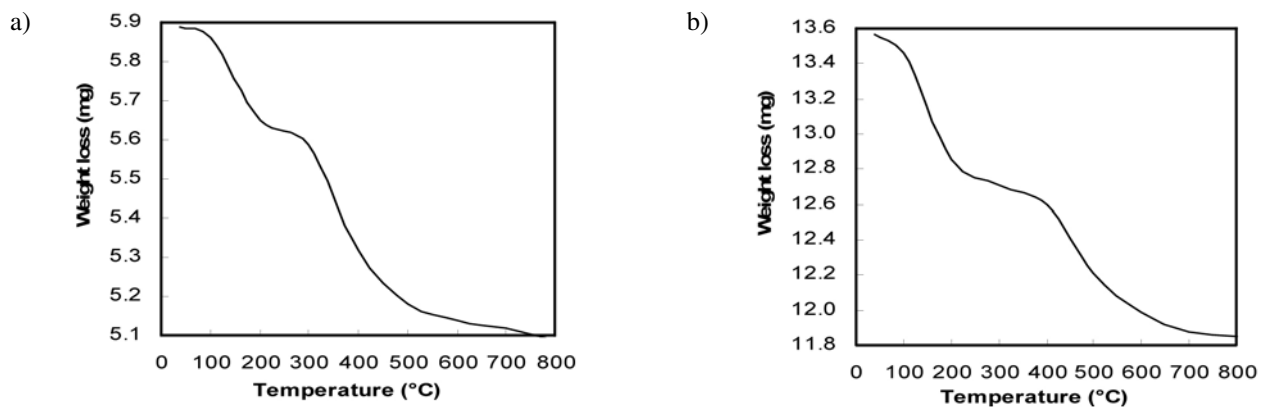


Fig. 3. Thermograms of (a) LiZTPA and (b) LiZTPC.

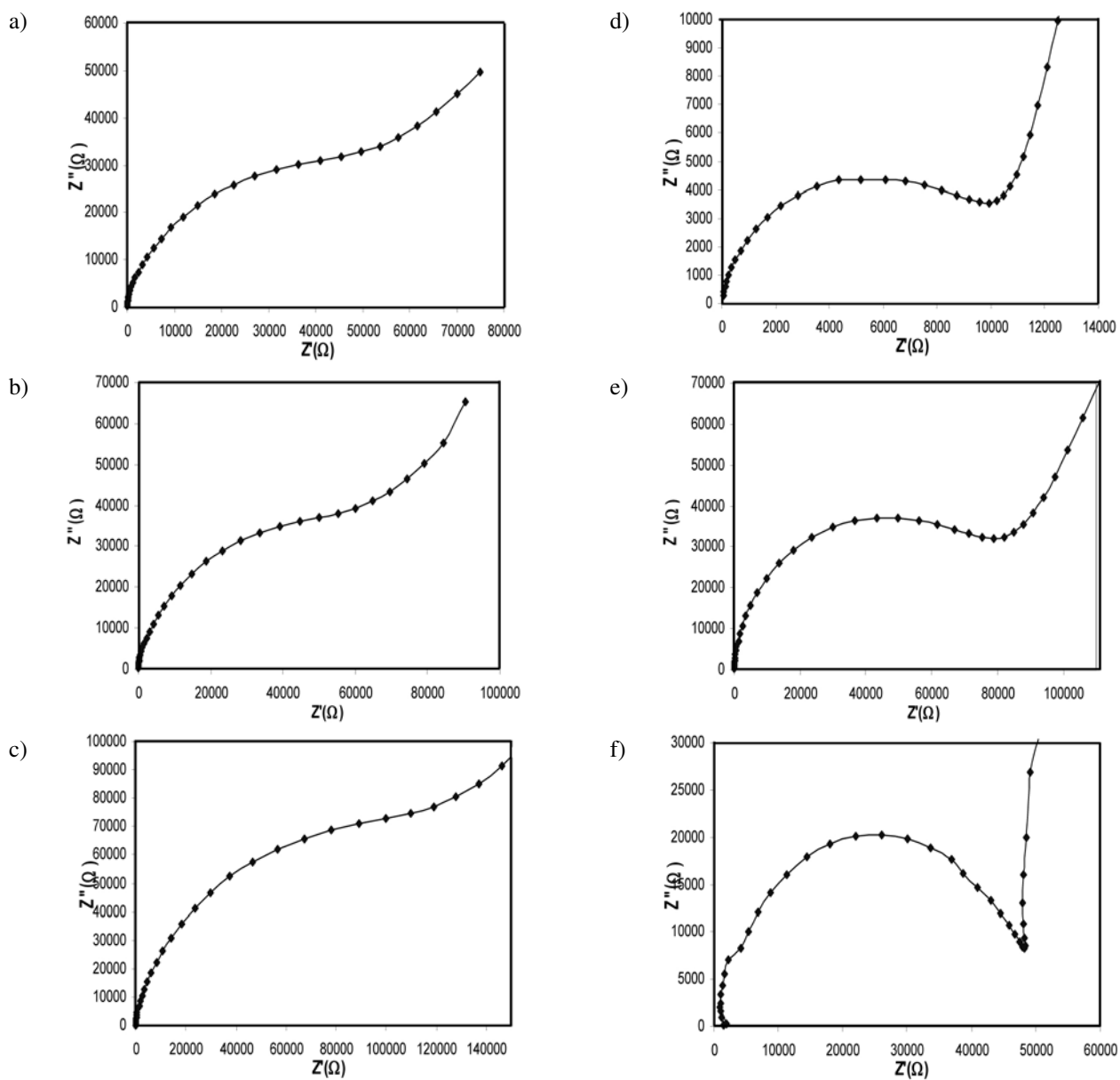


Fig. 4. Complex impedance plots for (a) LiZPA, (b) LiTPA (c) LiZTPA, (d) LiZPC, (e) LiTPC and (f) LiZTPC at 30 °C.

H<sub>2</sub>O respectively. The number of water molecules in each case was calculated using Alberti and Torracca formula.<sup>17</sup>

### 3. 2. Impedance Measurements

The complex impedance plots for LiZPA, LiTPA, LiZTPA, LiZPC, LiTPC, LiZTPC at 30 °C have been presented in Fig. 4a–f.

In all cases, the impedance spectrum consists of a single depressed semicircle attributed to the bulk electrolyte resistance. A low frequency tail observed is attributed to electrode – pellet interfacial impedance, indicating that the electronic conductivity is quite small/negligible<sup>18,19</sup>. The sample resistance ( $R$ ) was measured by extrapolation of the high frequency arc crossing to the  $Z$  (real) axis. The proton conductivity was measured using the equation,  $\sigma = l / RA$ , where  $\sigma$  is the conductivity (S cm<sup>-1</sup>),  $l$  is the thickness of the sample (cm) and  $A$  is the electrode area (cm<sup>2</sup>). The values of the activation energy  $E_a$  for each of the samples was calculated using the Arrhenius equation  $\sigma = \sigma_0 \exp(-E_a / kT)$ , where  $k$  is Boltzmann's constant and  $T$  is temperature. The results of specific conductance ( $\sigma$ ) and activation energy ( $E_a$ ) have been presented in Table 1.

( $\sim 10^{-5}$ – $10^{-6}$ ) in the temperature range 30–250 °C. However, at higher temperatures, TMA salts themselves give disordered complex impedance plots. Similar observations have been made earlier by us and other workers.<sup>7–9, 12</sup>

Proton conduction study of M(IV) phosphates shows that surface protons conduct  $\sim 1000$  times faster than bulk protons. The transport of protons (H<sup>+</sup>) between relatively stationary host anions is termed the 'Grotthuss' or 'free-proton' mechanism.<sup>20</sup> The Grotthuss mechanism requires close proximity of water molecules, which are firmly held but able to rotate. At temperature > 150 °C, the conduction is essentially due to bulk protons.<sup>21</sup> At this temperature, solid is anhydrous and the protons are covalently bonded to phosphate.<sup>22</sup> Thus, conduction of protons requires breaking and making of bonds. Thus, conduction decreases with increase in temperature as observed in the present study. In synthesizing lithium exchanged phases, it is well known that all sites cannot be exchanged with lithium.<sup>10,11</sup> Thus, exchanged phases contain two types of ions available for conduction and net/observed conductance is explained due to contribution of the two type of ions, viz. H<sup>+</sup> and Li<sup>+</sup>. At low temperature, the conduction is predominantly protonic, due to presence of zeolitic water (Grotthuss mechanism) and decreases with increase in temperature. The

**Table 1.** Specific conductivity  $\sigma$  (S cm<sup>-1</sup>) of LiZPA, LiTPA, LiZTPA, LiZPC, LiTPC, LiZTPC.

	Specific conductivity ( $\sigma$ ) S cm <sup>-1</sup> × 10 <sup>5</sup>					
	$\sigma_{\text{LiZPA}}$	$\sigma_{\text{LiTPA}}$	$\sigma_{\text{LiZTPA}}$	$\sigma_{\text{LiZPC}}$	$\sigma_{\text{LiTPC}}$	$\sigma_{\text{LiZTPC}}$
30	0.99	8.80	9.26	0.72	1.97	9.88
40	0.79	7.88	8.51	0.60	0.79	9.51
50	0.61	6.07	7.71	0.53	0.47	9.39
60	0.40	5.19	6.94	0.42	0.41	9.07
70	0.39	3.97	6.09	0.22	0.32	8.49
80	0.38	3.65	5.31	0.16	0.30	7.72
90	0.31	3.12	4.73	0.10	0.28	7.09
100	0.27	2.57	4.15	0.10	0.27	6.51
110	0.22	2.20	3.77	0.10	0.26	5.84
120	0.19	1.87	3.30	0.09	0.25	5.13
130	0.17	1.32	2.94	0.08	0.24	3.84
140	0.15	1.01	2.75	0.07	0.22	2.92
150	0.17	1.42	2.86	0.08	0.23	3.02
200	0.30	3.11	4.56	0.14	0.24	3.37
250	0.57	5.26	6.34	0.39	1.26	6.91
$E_a$ (kJ.mol <sup>-1</sup> ) in the range 90–120 °C	16.08	17.04	10.88	0.88	2.26	9.67
$E_a$ (kJ.mol <sup>-1</sup> ) in the range 140–250 °C	25.37	30.14	17.92	30.86	29.31	16.75

For all the materials, it is observed that specific conductivity decreases with increasing temperature upto 140 °C and then increases at higher temperatures. At a temperature as high as 250 °C the conductivity value is of the order of  $10^{-5}$ – $10^{-6}$  S cm<sup>-1</sup>. Complex impedance plot of lithium exchanged phases at 250 °C, exhibits a semicircular behaviour. The conductance values also remain constant

second, high temperature conduction, above 150 °C is due to the mobility of Li<sup>+</sup> that increases with increase in temperature. Since, H<sup>+</sup> is smaller in size than Li<sup>+</sup>, O–Li bond is weaker than O–H bond, it is anticipated that Li–O framework bond allows faster lithium conductance. As temperature increases, the mobility of lithium ion also increases which explains higher conduction above 150 °C.

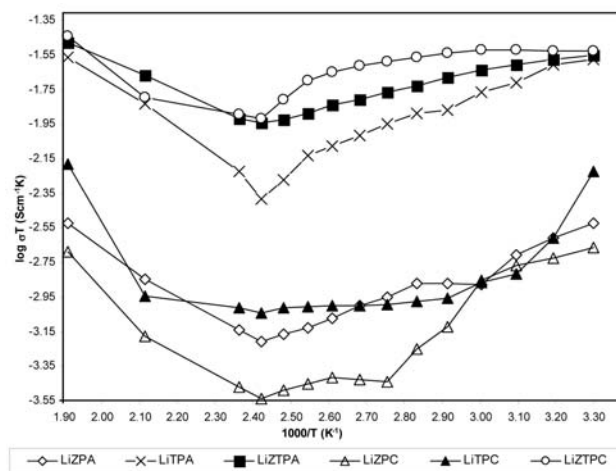


**Fig 5.** Arrhenius plots for (a) LiZPA, (b) LiTPA (c) LiZTPA, (d) LiZPC, (e) LiTPC and (f) LiZTPC in temperature range 30–250 °C.

Arrhenius plots ( $\log \sigma T$  vs  $1/T$ ) in the temperature range 30–250 °C have been presented in Fig. 5. In general, for all the materials, transition from proton to lithium ion conduction occurs in the region  $\sim 140$  °C. Energy of activation ( $E_a$ ) values calculated in the temperature range 90–120 °C and 140–250 °C are presented in Table 1. From Table 1, it is observed that,  $E_a$  values are higher in 140–250 °C region as compared to 90–120 °C region.  $H^+$  being lighter than  $Li^+$ ,  $E_a$  values are expected to be higher for  $Li^+$  as compared to  $H^+$ , indicating conduction to be predominantly due to  $Li^+$  in the high temperature region (140–250 °C) and due to  $H^+$  in the low temperature region (90–120 °C). Lower  $E_a$  values in the 90–120 °C region, indicate ease of conduction and suggests the mechanism to be Grotthuss type, where  $E_a$  entirely depends on reorientation of water molecules on the surface, which has been explained earlier in the text. Further, low  $E_a$  values 17.92 and 16.75  $\text{kJ mol}^{-1}$  for LiZTPA and LiZTPC respectively compared to their single salt counterparts also indicates ease of lithium conduction.

It is observed that, in cases of both amorphous and crystalline phases, titanium phosphate (TP) exhibits greater conductance compared to zirconium phosphate (ZP). It is observed<sup>23,24</sup> that at 30 °C,  $\sigma_{TP(\text{amorphous})} (4.03 \times 10^{-5} \text{ Scm}^{-1}) > \sigma_{ZP(\text{amorphous})} (2.30 \times 10^{-6} \text{ Scm}^{-1})$  as well as  $\sigma_{TP(\text{crystalline})} (9.09 \times 10^{-6} \text{ Scm}^{-1}) > \sigma_{ZP(\text{crystalline})} (6.56 \times 10^{-6} \text{ Scm}^{-1})$ . Since both ZP and TP have a common anion  $HPO_4^{2-}$ , the conductivity of the materials should bear a correlation with the acidity of the cations. Acidity of a cation is related to ion size and charge. Ionic radii for  $Ti^{4+}$  is 0.745 Å and  $Zr^{4+}$  is 0.86 Å.<sup>25</sup>  $Ti^{4+}$  with a high charge density exhibits greater proton conductivity. In the present work, for both amorphous and crystalline phases,  $\sigma_{LiTP} > \sigma_{LiZP}$ . Clearfield et al<sup>26</sup> have also studied the lithium exchanged phases of crystalline zirconium phosphate, in which  $Zr^{4+}$  is progressively substituted by  $Ti^{4+}$  and observed increased conductance. They have explained increased conduc-

tance to be due to decrease in cavity sizes upon substitution. This causes  $Ti^{4+}$  and  $Li^+$  to be in close proximity, which leads to repulsion between them leading to weaker Li–O bond and hence higher conductance. There is therefore, critical interplay of several factors responsible for conductivity.

Further, for both amorphous and crystalline phases, the order of specific conductance at 30 °C is  $-\sigma_{LiZTP} > \sigma_{LiTP} > \sigma_{LiZP}$ . This is as per our earlier observations in case of TMA salts, that mixed materials exhibit higher conductance compared to their single salts counterparts.<sup>14,23,24</sup> Higher specific conductivity of mixed materials may be attributed to some structural changes. However, as discussed above, the final conductance is a critical interplay of several factors.

## 4. Conclusions

In lithium exchanged phases of TMA salts, conductance is due to contribution of both  $H^+$  as well as  $Li^+$ . This conductance is also retained up to fairly higher temperature due to high mobility of  $Li^+$  ion at high temperature. Thus the study reveals the importance of lithium-exchanged phases of TMA salts as solid electrolyte for medium and high temperature applications.

## 5. References

- 1 W. H. J. Hogarth, J. C. Diniz da Costa and G.Q. Lu(Max), *J. Power Sources*, **2005**, *142*, 223–237.
- 2 I. A. Stenina, A. D. Aliev, P. K. Dorhout, A. B. Yaroslavtsev, *Inorg. Chem.*, **2004**, *43*, 7141–7145.
- 3 M. Casciola, D. Fabiani, *Solid State Ionics*, **1983**, *11*, 31–38.
- 4 K. Nomura, S. Ikeda, K. Ito, H. Einaga, *Solid State Ionics*, **1993**, *61*, 293–301.
- 5 L. Szirtes, J. Megyeri, L. Riess, E. Kuzmann, *Solid State Ionics*, **2003**, *162–163*, 181–184.
- 6 M. Mizuhata, F. Ito, S. Deki, *J. Power Sources*, **2005**, *146*, 365–370.
- 7 J. R. Ramos-Barrado, C. Criado, P. Maireles-Torres, P. Oliveira-Pastor, E. Rodríguez-Castellón, A. Jimenez-Lopez, *Solid State Ionics*, **1994**, *73*, 67–73.
- 8 C. Criado, J. R. Ramos Barrado, P. Maireles-Torres, P. Oliveira-Pastor, E. Rodríguez Castellón and, A. Jiménez-López, *Solid State Ionics*, **1993**, *61*, 139–142.
- 9 J. R. Ramos-Barrado, F. Martín, E. Rodriguez-Castellón, A. Jimenez-López, P. Olivera-Pastor, F. Pérez-Reina, *Solid State Ionics*, **1997**, *97*, 187–194.
- 10 Gregory A. Becht, John T. Vaughey, Robin L. Britt, Cassandra T. Eagle, Shiou-Jyh Hwu, *Mater. Res. Bull.*, **2008**, *43*, 3389–3396.
- 11 S. Poisson, F. d'Yvoire, N. Nguyen-Huy-Dung, E. Bretey, P. Berthet, *J. Solid State Chem.*, **1998**, *138*, 32–40.
- 12 R. Thakkar, H. Patel, U. Chudasama, *Bull. Mater. Sci.*, **2007**, *30*, 205–209.

- 13 G. Alberti, M. Casciola, U. Constantino, M. Leonardi, *Solid State Ionics*, **1984**, *14*, 289–295.
- 14 B. Beena, U. Chudasama, *Bull. Mater. Sci.*, **1996**, *19*, 405–409.
- 15 R.C.T. Slade, J. A. Knowels, D. J. Jones, J. Roziere, *Solid State Ionics*, **1997**, *96*, 9–19.
- 16 J. W. Robinson, *Handbook of Spectroscopy*, CRC press, Ohio, **1974**, pp. 99–101.
- 17 G. Alberti, E. Torracca, *J. Inorg. Nucl. Chem.*, **1968**, *30*, 3075–3080.
- 18 E. Jaimez, G. B. Hix, R. C. T. Slade, *Solid state Ionics*, **1997**, *97*, 195–201.
- 19 Zhi Ping Xu, Youggay Jin, Joe C. Dinno da Costa, *Solid state Ionics*, **2008**, *178*, 1654–1659.
- 20 A. Clearfield and P. Jerus, *Solid State Ionics*, **1982**, *6*, 79–83.
- 21 C. J. D. Grothuss, *Ann. Chim.*, **1806**, *58*, 54–73.
- 22 J. M. Troup and A. Clearfield, *Inorg. Chem.*, **1977**, *16*, 3311–3314.
- 23 R. Thakkar and U. Chudasama, *Electrochimica Acta*, **2009**, *54*, 2720–2726.
- 24 R. Thakkar and U. Chudasama, *Electrochim. Acta*, **2009**, *54*, 2720–2726.
- 25 R. Shannon, *Acta Crystallogr.*, **1976**, *32*, 751–767.
- 26 M. A. Subramanian, R. Subramanian, A. Clearfield, *Solid State Ionics*, **1986**, *18–19*, 562–569.

## Povzetek

Litijeve izmenjane faze amorfne in kristaliničnega cirkonijevega titanovega fosfata smo sintetizirali s tehniko ionske izmenjave. Materiale smo karakterizirali z elementno analizo (ICP-AES in AAS), spektroskopijo (FTIR), termično analizo (TGA) in rentgensko fazno analizo. Prevodnost sintetiziranih materialov smo raziskovali z merjenjem specifične prevodnosti z impedančnim analizatorjem v temperaturnem območju med 30 in 250 °C v frekvenčnem območju od 1 Hz – do 32 MHz pri napetosti, manjši od 1 V. Litijeve izmenjane faze amorfne in kristaliničnega cirkonijevega fosfata in titanovega fosfata smo sintetizirali pod enakimi pogoji in za primerjavo merili njihovo prevodnost. V vseh primerih prevodnost fosfatnih materialov pada z naraščajočo temperaturo.